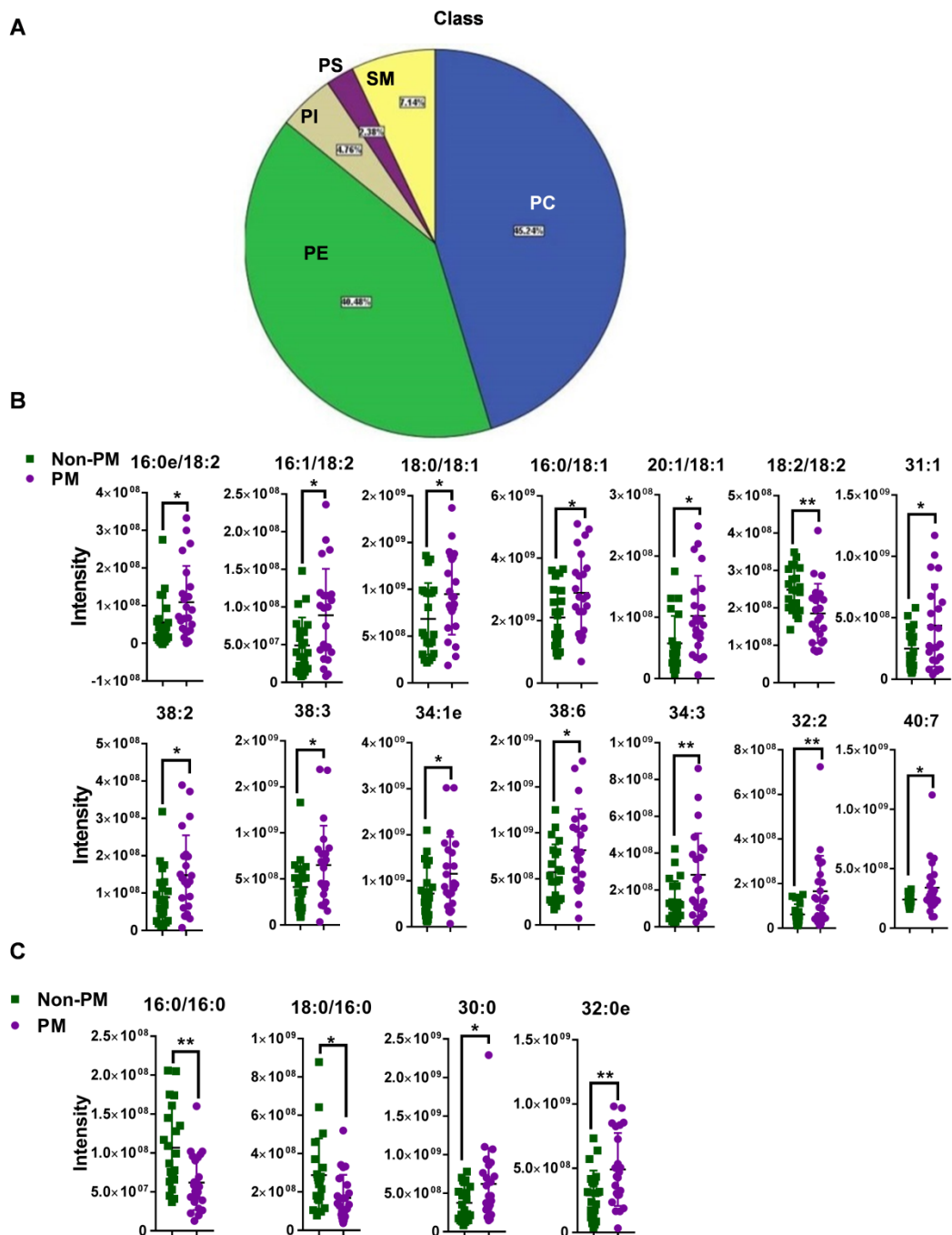


## Supplementary figures and figure legends

Figure S1



**Figure S1. Altered lipids in clinical CRC specimens detected by lipidomics. A,** Pie chart of lipid classes whose abundance was significantly changed. **B-C,** Intensity of phosphatidylcholine (PC) with unsaturated acyl chains (**B**) and saturated acyl chains (**C**) from clinical CRC specimens. PM, n=23; nPM, n=22. p < 0.05; \*\*, p < 0.01.

Figure S2

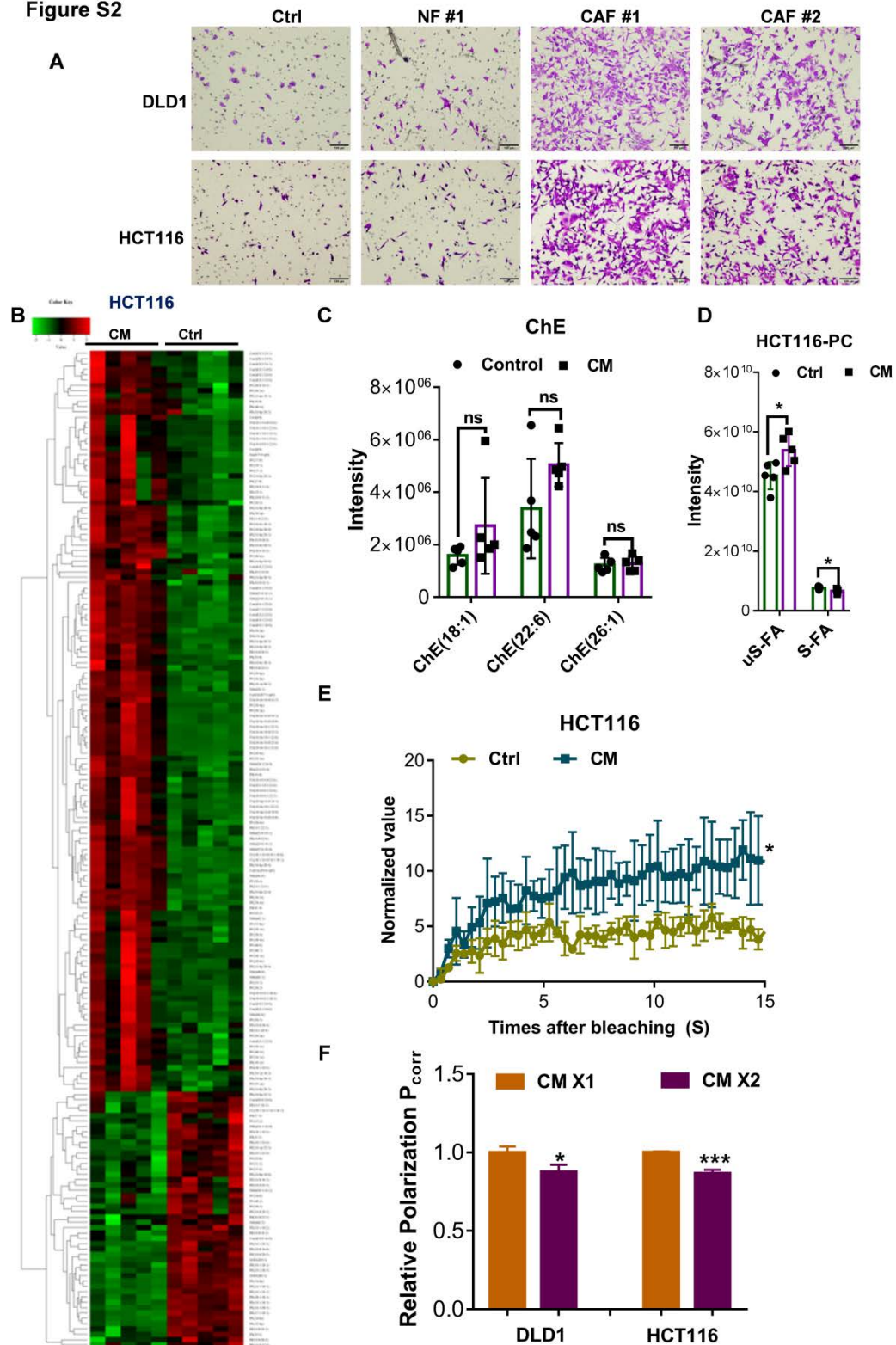
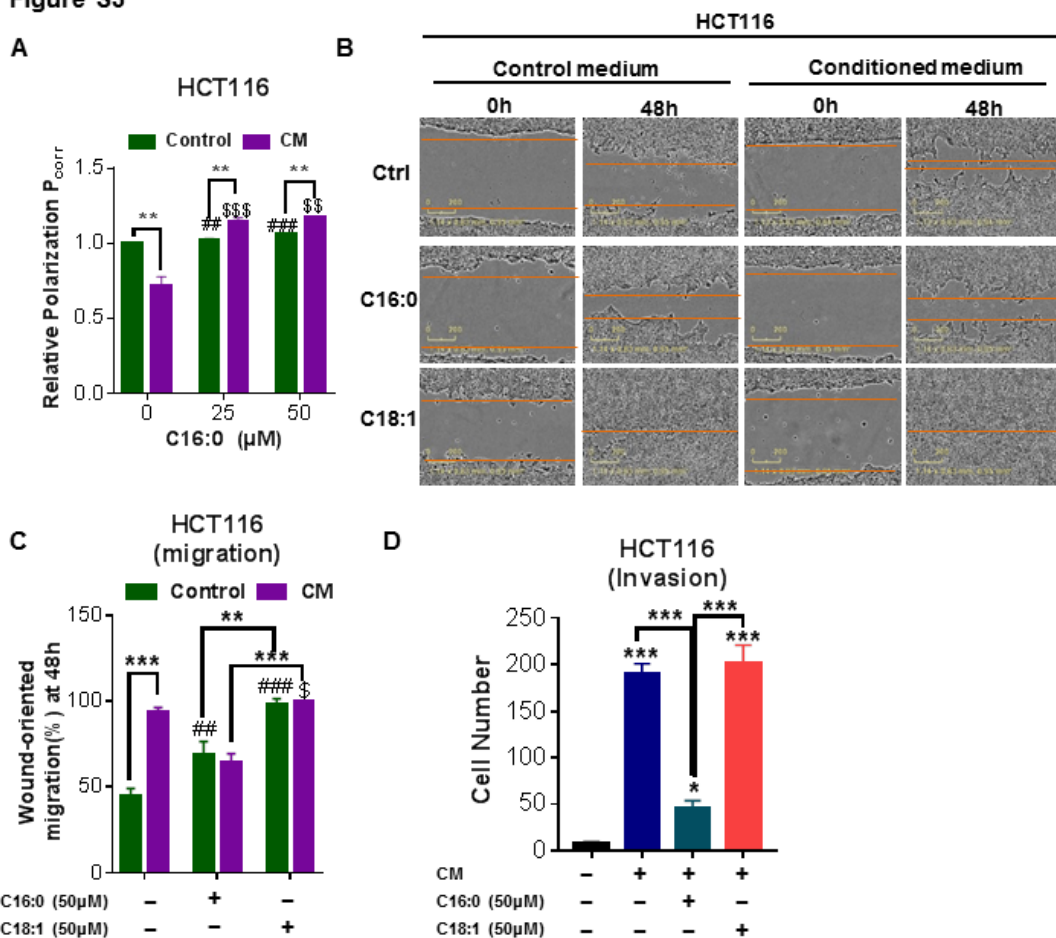


Figure S2. CAFs increased phosphatidylcholine (PC) with acyl chain unsaturation and membrane fluidity in CRC cells. **A**, Crystal violet staining to quantify the Transwell invasion of the indicated cells after 24 h of exposure to CAF-CM or NF-CM. NF, Normal fibroblast. **B**, Heat map of altered lipids in

CAF-CM-treated HCT116 cells detected by lipidomics. CAF-CM as detected by IncuCyte ZOOM. **C**, ChE (steroid) distribution in CAF-CM-incubated HCT116 cells. n=5. **D**, Intensity of PC containing saturated acyl chains and unsaturated acyl chains in CAF-CM-incubated HCT116 cells. n=5. **E**, Normalized fluorescence recovery curve of HCT116 cells cultured with control/conditioned medium. n = 3. **F**, Fluorescence polarization (Relative Polarization<sub>corr</sub>) in CRC cells incubated with 25% CAF-CM or a double dose of CAF-CM (50%). n = 2 independent experiments with 2 CAF-CM samples from different CAF cell lines. Bars, mean ± SD. \*, p < 0.05, \*\*\*, p < 0.001.

**Figure S3**



**Figure S3. C16:0 inhibits CRC cell migration and invasion by decreasing membrane fluidity.** **A**, Fluorescence polarization (Relative Polarization<sub>corr</sub>) in CAF-CM/C16:0-treated HCT116 cells. **B**, Wound healing assay of HCT116 cells incubated with CAF-CM and treated with the indicated compounds as detected by IncuCyte ZOOM. n=3. **C**, Quantification of the wounding rates of HCT116 cells in **(B)**. # and \$ indicate comparisons with the corresponding

control groups. Wound width was normalized to the initial width when the wound was created. n=3. **D**, The number of crystal violet-stained cells among HCT116 cells that invaded the Transwell. n=3. Bars, mean  $\pm$  SD. n=3 \*, \$ p < 0.05; \*\*, ##, \$\$ p < 0.01; \*\*\*, ###, \$\$\$ p < 0.001.

Figure S4

DLD1

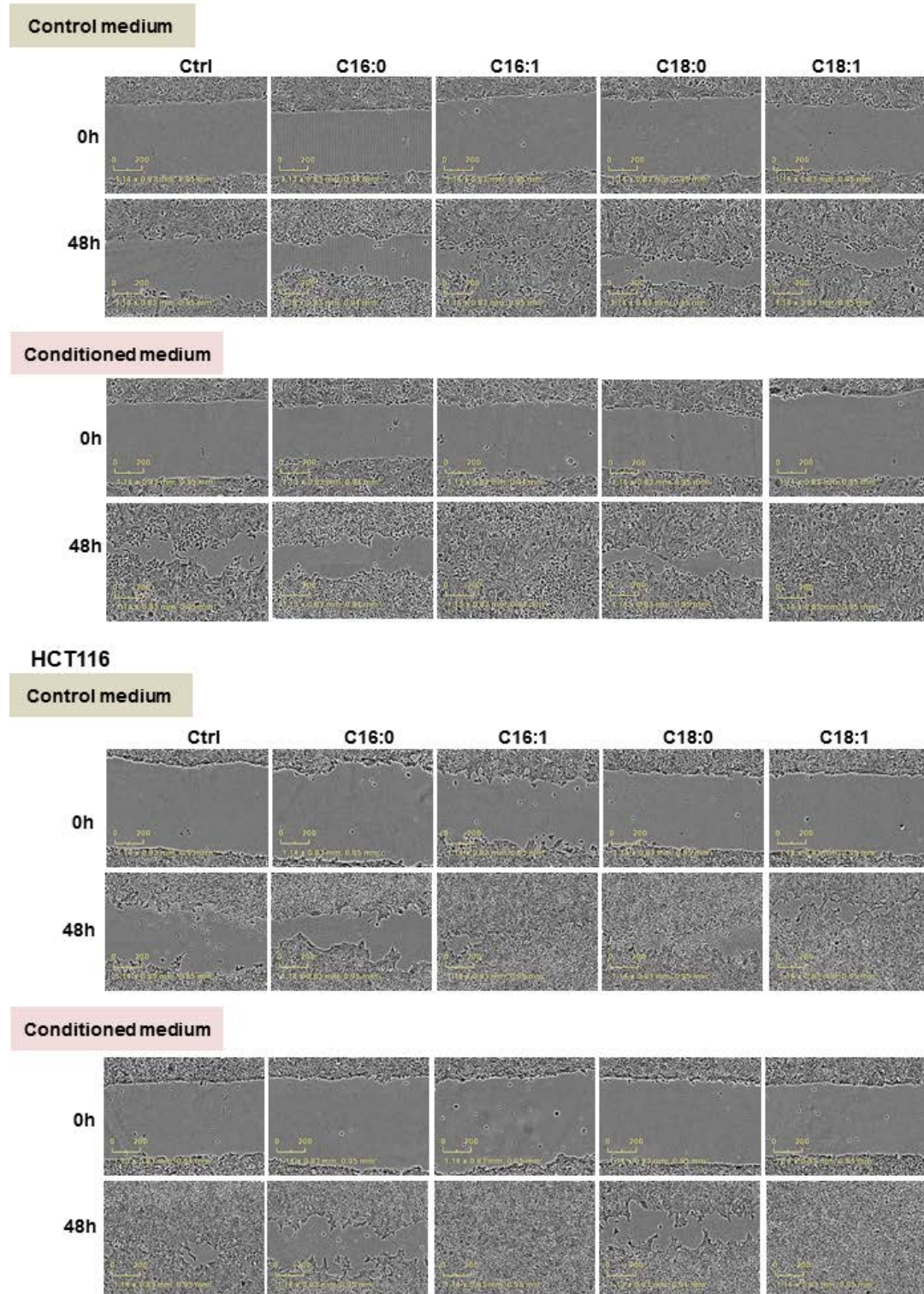


**Figure S4. S-FAs inhibit CRC cell migration.** Wound healing assay of DLD1/HCT116 cells incubated with CAF-CM and treated with the indicated compounds as detected by IncuCyte ZOOM. n = 2 independent experiments

with 2 CAF-CM samples from different CAF cell lines.

Figure S5

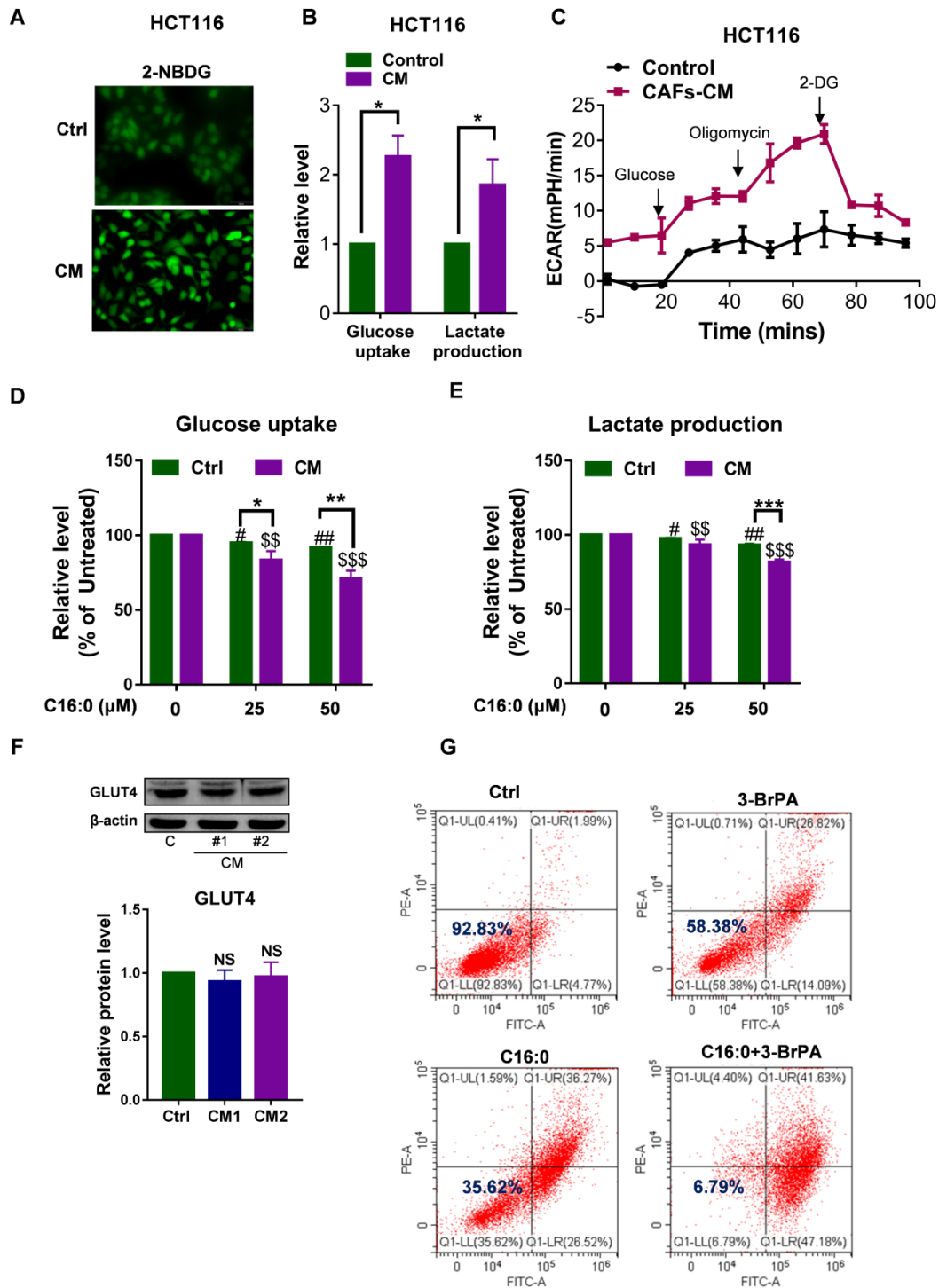
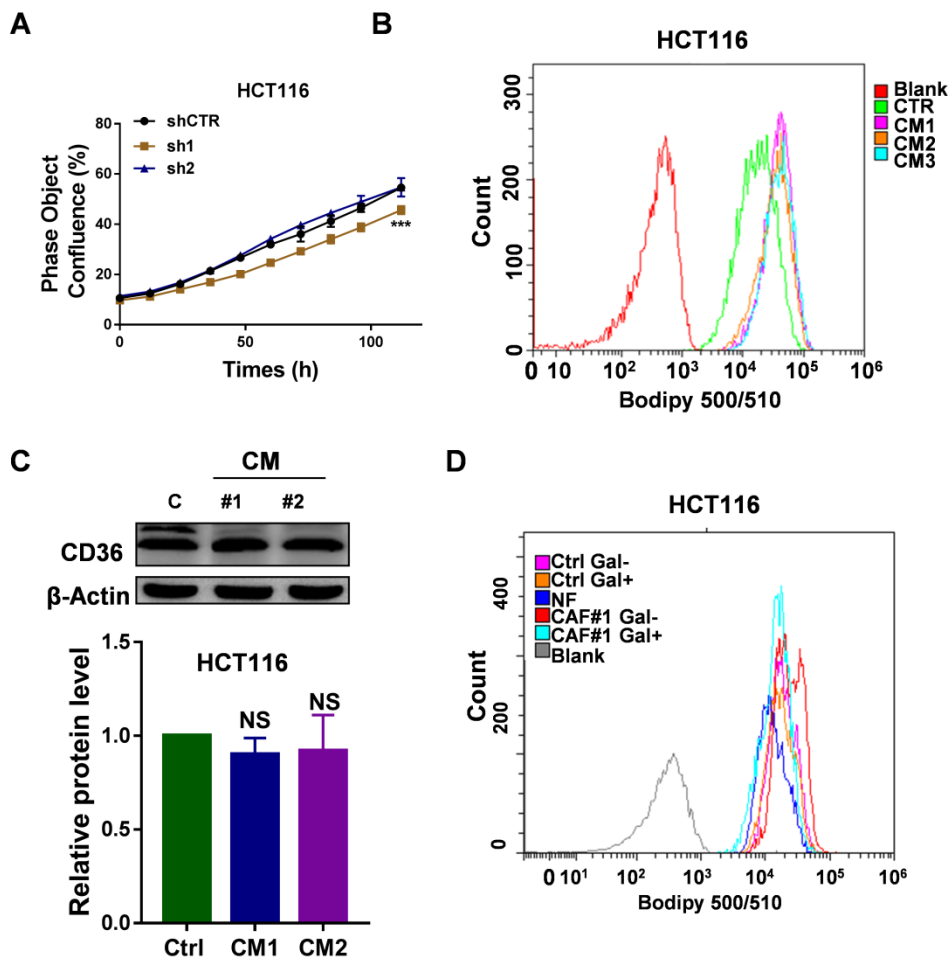


Figure S5. Increased cell membrane fluidity enhances glucose uptake and metabolism. A, Glucose uptake by HCT116 cells incubated with CAF-

CM or control medium, as visualized by 2-NBDG fluorescence.  $n=3$ . **B**, Relative levels (% of control) of glucose uptake and lactate production in HCT116 cells after incubation with CAF-CM.  $n=3$ . **C**, Impact of CAF-CM incubation on the extracellular acidification rate (ECAR). The ECAR of HCT116 cells was monitored using a Seahorse XF24 analyzer.  $n=2$  independent experiments with similar results. **D-E**, Glucose uptake (D) and lactate production (E) in CAF-CM-treated HCT116 cells cultured in the absence or presence of C16:0 (concentration from 0 to 50  $\mu\text{M}$ ).  $n=3$ . **F**, The protein level of GLUT4 in CAF-CM-treated DLD1 cells was assessed by Western blotting.  $n=3$ . **G**, The viability of HCT116 cells incubated with CAF-CM was assessed by annexin-V/PI assay after 48 h incubation with 3-BrPA. The value in each panel indicates the % of surviving cells.  $n=2$  independent experiments with similar results. Bars, mean  $\pm$  SD. \*, #  $p < 0.05$ ; \*\*, ##, \$\$  $p < 0.01$ ; \*\*\*, \$\$\$  $p < 0.001$ .

**Figure S6**



**Figure S6. CAF-derived lipids boosted CRC growth and metastasis.**

**A**, The proliferation rate of HCT116<sup>low-SCD</sup> cells, as evaluated by phase object confluence (%) with IncuCyte ZOOM. n=3. **B**, HCT116 cells treated as indicated were incubated with BODIPY 500 (lipid uptake). The cells were analyzed by flow cytometry. **C**, Western blot showing CD36 expression in HCT116 cells incubated with CAF-CM. **D**, The HCT116 cells treated with indicated CM were incubated with BODIPY 500/510 to analyze lipid uptake by flow cytometry. Bars, mean  $\pm$  SD. \*\*\*p < 0.001; NS, not statistically significant.

**Figure S7**

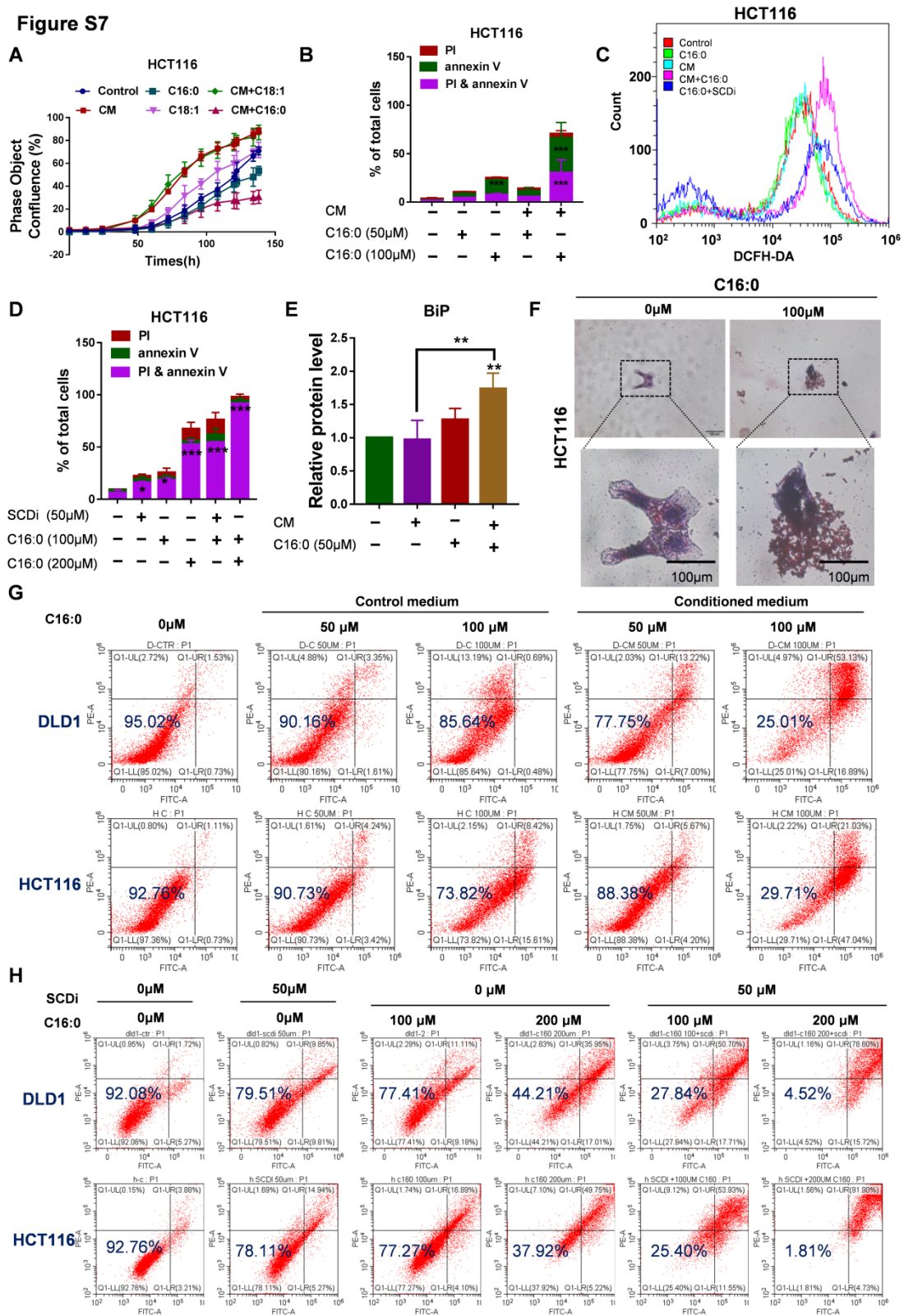


**Figure S7. Treatment of cells with C16:0 increased lipotoxicity-induced CRC cell apoptosis. A, Growth curve of HCT116 cells treated with the indicated compounds. IncuCyte ZOOM software was used to process the image data for phase object confluence. n=3. B, C16:0 induces apoptotic cell**

death in HCT116 cells. Cell viability assay of HCT116 cells treated with different concentrations of C16:0 (0, 50 and 100  $\mu$ M) for 48 h. Apoptotic cells were identified by propidium iodide (PI) and annexin V staining. n=3. **C**, Reactive oxygen species (ROS) levels in HCT116 cells with or without CAF-CM incubation and SCD inhibitor treatment were detected by flow cytometry. n = 2 independent experiments with similar results. **D**, SCD inhibitor treatment increased HCT116 cell sensitivity to C16:0. Cell viability was assessed by annexin-V/PI assay. n=3. **E**, Relative protein level of BIP (GRP78 BiP) in HCT116 cells incubated with CAF-CM or after C16:0 treatment (50  $\mu$ M, ~6 h) determined by Western blotting. Anti-BIP antibody (1:1000 dilution; Abcam, Cambridge, MA, USA), n=3. **F**, HCT116 cells incubated with CAF-CM and then treated with C16:0 were detected by oil red/hematoxylin staining. The cells were imaged using an inverted microscope. n = 3. **G-H**, FACS was used to detect the apoptosis of the indicated cells. Bars, mean  $\pm$  SD. \*, p < 0.05; \*\*, p < 0.01; \*\*\*, p < 0.001.

**Figure S8**

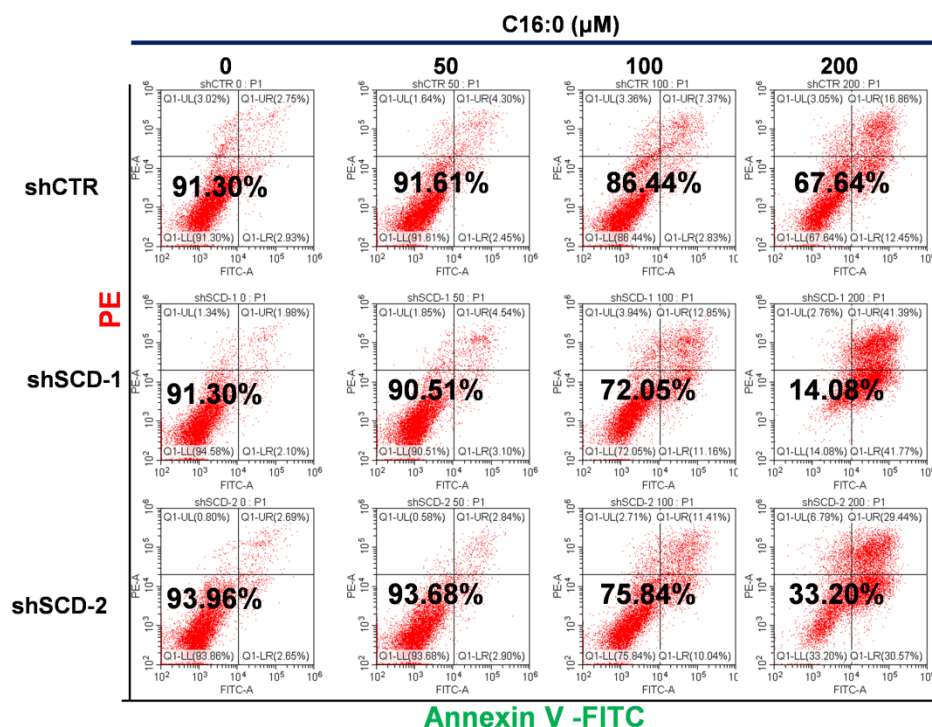
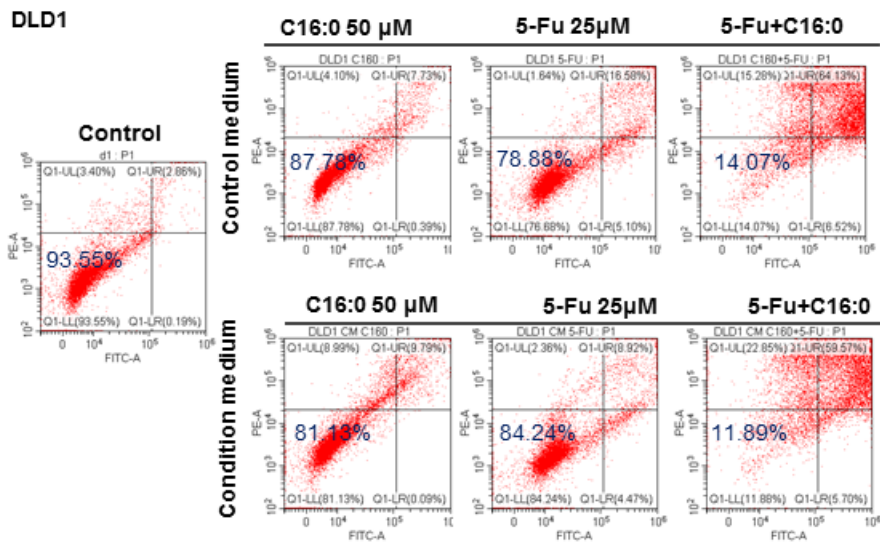


**Figure S8. High doses of palmitate aggravated the lipotoxicity of CRC<sup>low</sup> SCD cells.** Cell viability assay of the indicated HCT116 cells treated with

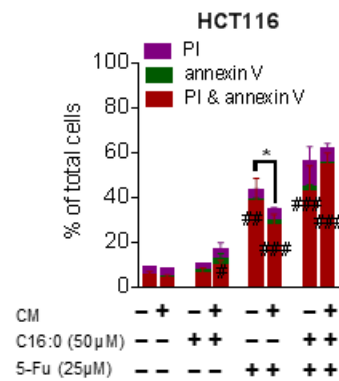
different concentrations of C16:0 (0, 50, 100 and 200  $\mu\text{M}$ ) for 48 h and then detected by the annexin-V/PI assay. Apoptotic cells were identified by propidium iodide (PI) and annexin V staining. n=3

Figure S9

A



B



C

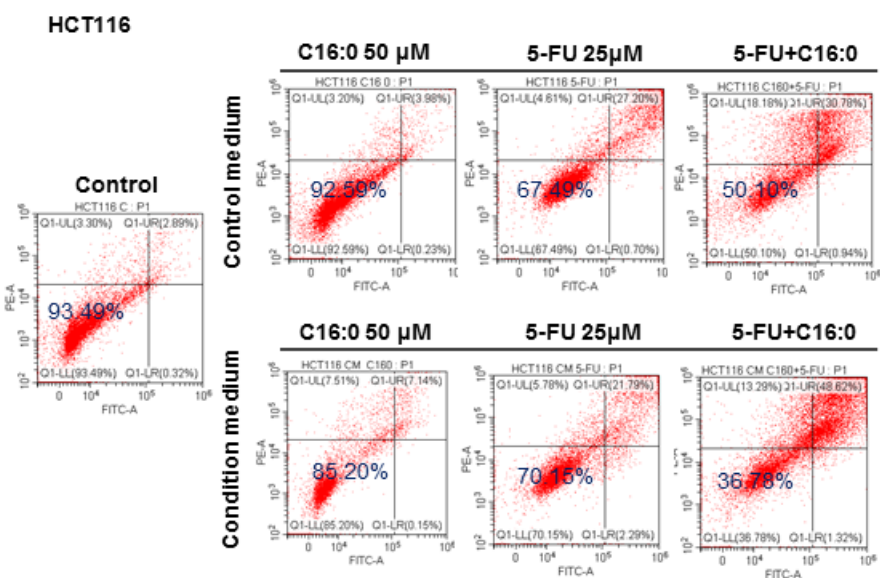


Figure S9. C16:0 acts synergistically with 5-FU to effectively kill CRC cells incubated with CAF-CM *in vitro*. A, FACS was used to detect the apoptosis of the indicated cells. DLD1 cells were treated with the indicated

concentration of C16:0/5-FU for 48 h and subjected to the annexin-V/PI assay. **B**, C16:0/5-FU induced apoptotic cell death in HCT116 cells. n=3. **C**, FACS was used to detect the apoptosis of the indicated cells. HCT116 cells were treated with the indicated concentration of C16:0/5-FU for 48 h and subjected to the annexin-V/PI assay. Bars, mean  $\pm$  SD. \*,  $p < 0.05$ ; \*\*,  $p < 0.01$ ; \*\*\*,  $p < 0.001$ .